

# Aggregate Morphology and Hydrogenation Reactivity of Functionalized Bilayer Membrane Composed of Peptide Lipid Having NADH Activity†

Yukito MURAKAMI,\* Jun-ichi KIKUCHI, Koji NISHIDA, and Akio NAKANO††

Department of Organic Synthesis, Faculty of Engineering, Kyushu University,

Hakozaki, Higashi-ku, Fukuoka 812

(Received December 19, 1983)

A peptide lipid bearing the 1,4-dihydronicotinamide moiety, *N,N*-dihexadecyl-*N*′-[1-(6-trimethylammoniohexyl)-1,4-dihydro-3-pyridylcarbonyl]-L-alaninamide bromide [ $N^+C_6(NAH)Ala2C_{16}$ ], and its dehydrogenated form, *N,N*-dihexadecyl-*N*′-[1-(6-trimethylammoniohexyl)pyridinium-3-ylcarbonyl]-L-alaninamide chloride bromide [ $N^+C_6(NA^+)Ala2C_{16}$ ], were prepared. Both lipids formed bilayer membranes when they were dispersed in aqueous media, and the 1,4-dihydronicotinamide and nicotinamide moieties of the respective lipid molecules were placed in the so-called hydrogen-belt domain upon membrane formation. In an aqueous dispersion of the latter dicationic lipid, relatively small multilayered vesicles were predominantly formed while the related monocationic lipids bearing the same double alkyl chain composed much larger vesicles and/or lamellae. Formation of the charge-transfer (CT) complex of the nicotinamide moiety of  $N^+C_6(NA^+)Ala2C_{16}$  with 3-indolylacetic acid was much enhanced in the membrane through tight electrostatic interaction. The bilayer membrane composed of  $N^+C_6(NAH)Ala2C_{16}$  acted as a potential reductant toward anionic substrates in aqueous media. The high reactivity is gained primarily by the effective incorporation of the substrates into the hydrogen-belt domain through electrostatic, hydrogen bonding, and CT interactions and partly by the proximity effect which becomes valid between the 1,4-dihydronicotinamide moiety and the bound substrate molecule.

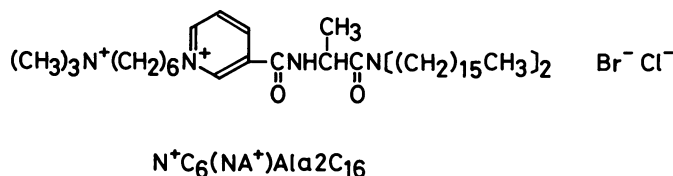
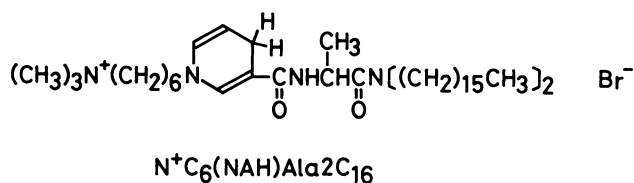
Currently, there is growing attention to the physical properties and aggregation behavior of synthetic lipids in aqueous media.<sup>1)</sup> Since synthetic bilayer membranes provide hydrophobic and organized microenvironments to various extents, it is of much interest to carry out various organic reactions in such organic media. Coenzyme NAD(P)H is one of the most frequently occurring cofactors for electron-transfer reactions in biological systems, and the activity of integral enzymes is often sensitive to the change in lipid composition of membranes where such enzymes are bound.<sup>2)</sup> Meanwhile, synthetic membranes may simulate the functions of apoproteins by providing hydrophobic and organized microenvironments for NAD(P)H.

We have previously clarified that peptide lipids compose stable bilayer vesicles having a tripartite structure: a hydrophobic zone formed with aliphatic double chains, a hydrophilic zone with ionic head groups, and

a hydrogen-belt domain with amino acid residues interposed between the former two zones.<sup>3,4)</sup> In addition, we have found that the hydrogen-belt domain serves as effective sites for hydrolysis and transamination reactions which simulate the functions of esterase and vitamin B<sub>6</sub>-dependent transaminase, respectively.<sup>5)</sup> In the present work, we prepared a peptide lipid bearing the 1,4-dihydronicotinamide moiety,  $N^+C_6(NAH)Ala2C_{16}$ . The lipid was so designed as to place the dihydronicotinamide moiety in the hydrogen-belt domain when the membrane is formed. In the light of the aggregate morphology of  $N^+C_6(NAH)Ala2C_{16}$  examined herein, we studied the reduction of various substrates with the single-compartment bilayer vesicles in aqueous media.

## Experimental

**General Analyses and Measurements.** Elemental analyses were performed at the Microanalysis Center of Kyushu University. Melting points were measured with a Yanagimoto MP-S1 apparatus (hot-plate type). <sup>1</sup>H-NMR spectra were taken on either a Hitachi R-24B or a Hitachi Perkin-Elmer R-20 spectrometer. pH-Measurements were carried out with a Beckman expandomatic SS-2 pH meter equipped with a Metrohm EA-125 combined electrode after calibration with a combination of appropriate standard aqueous buffers. Fluorescence and electronic absorption spectra were obtained with a Hitachi 650-60 spectrofluorometer and a Union Giken SM-401 high-sensitivity spectrophotometer, respectively. Rapid reactions between the 1,4-dihydronicotinamide moiety and substrates were monitored with a Union Giken RA-401 stopped-flow spectrophotometer. The fluorescence polarization measurements were made on a Union Giken FS-501A fluorescence polarization spectrophotometer equipped with a Sord microcomputer M200 Mark II; the emission at 449 nm was monitored upon excitation at 360 nm with a slit width of 3.5 nm for both excitation and emission sides. The fluorescence polarization (*P*) was calculated by Eq. 1, where *I* is the fluorescence intensity, and



† Contribution No. 719 from this Department.

†† Present address: Department of Food Science, Toa University, Shimonoseki, Yamaguchi 751.

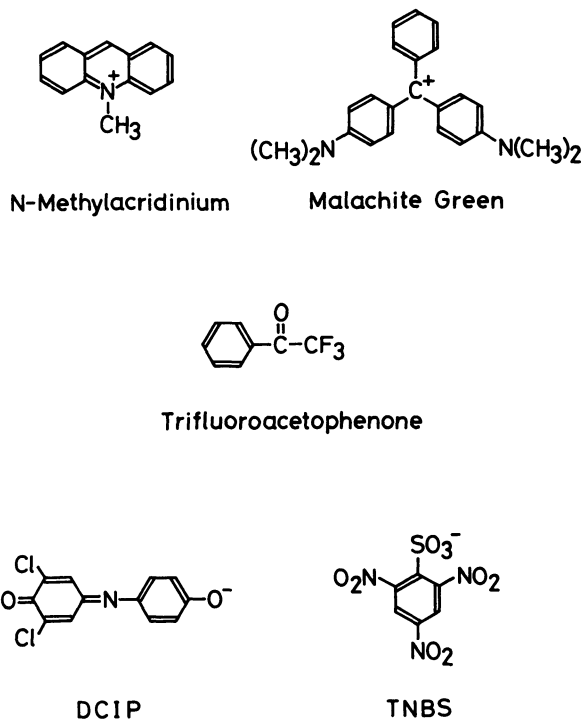
the subscripts v and h refer to the orientations, vertical and horizontal, respectively, for the excitation and analyzer polarizers in this sequence; e.g.,  $I_{vh}$  indicates the fluorescence intensity measured with a vertical excitation polarizer and a horizontal analyzer polarizer.<sup>6)</sup>

$$P = (I_{vv} - C_f I_{vh}) / (I_{vv} + C_f I_{vh}). \quad (1)$$

$C_f$  is the grating correction factor, given by  $I_{hv}/I_{hh}$ . A JEOL JEM-200B electron microscope, installed at the Research Laboratory for High Voltage Electron Microscopy of Kyushu University, was used for morphological measurements. The detail of sample preparation for electron microscopy has been described elsewhere.<sup>4)</sup>

**Differential Scanning Calorimetry (DSC).** The phase transition temperature ( $T_m$ , temperature at a peak maximum of DSC thermogram) for an amphiphile was measured with a differential scanning calorimeter (Daini Seikosha SSC-560U): heating rate, 2°C/min; chart speed, 0.5 cm/min; sensitivity, 0.025 mcal/s/(full scale); temperature and transition heat being calibrated with benzophenone (48°C) and/or water (0°C). Each 50-μl sample of an aqueous dispersion [2.0 (w/w)%] in redistilled and deionized water was weighed and sealed into a silver capsule. The enthalpy change for phase transition ( $\Delta H$ ) was determined by measuring the peak area of DSC thermogram.

**Materials.** Sodium 2,4,6-trinitrobenzenesulfonate (TNBS), 2,6-dichloroindophenol (DCIP) (both from Wako Pure Chemical Industries), and Malachite Green (Merck) were obtained from commercial sources as guaranteed reagents and used without further purification. *N*-Methylacridinium chloride<sup>7)</sup> and trifluoroacetophenone<sup>8)</sup> were prepared according to the procedures reported in literature, and the products were identified by various spectroscopic measurements.



*N,N*-Dihexadecyl-*N*<sup>a</sup>-nicotinoyl-L-alaninamide [(NA)Ala-2C<sub>16</sub>].

Trifluoroacetic acid (25 g, 220 mmol) was added to a dry dichloromethane solution (20 ml) of *N,N*-dihexadecyl-*N*<sup>a</sup>-(*t*-butoxycarbonyl)-L-alaninamide<sup>9)</sup> (6.0 g, 9.4 mmol), and the mixture was stirred for 30 min at room temperature. Evaporation of an excess amount of trifluoroacetic

acid *in vacuo* gave a pale brown oil. Elimination of the *t*-butoxycarbonyl group was confirmed by <sup>1</sup>H-NMR spectroscopy. The amine thus formed was dissolved in dry benzene (20 ml), and the solution was cooled to 0°C. Triethylamine (6.0 g, 60 mmol) was added dropwise to the solution, and then nicotinoyl chloride (3.7 g, 26 mmol) dissolved in dry benzene (20 ml) was added dropwise to the mixture in 20 min at 0°C with stirring. The resulting mixture was stirred for 30 min at 0°C and then washed with saturated aqueous sodium chloride (3×50 ml). After being dried over Na<sub>2</sub>SO<sub>4</sub>, the solution was evaporated to dryness *in vacuo*. The residue was chromatographed on a column of silica gel (Wako gel C-100) with ethyl acetate as an eluant. Evaporation of the solvent gave a pale brown solid: yield 4.5 g (75%); <sup>1</sup>H-NMR (CDCl<sub>3</sub>, TMS)  $\delta$ =0.88 [6H, t, (CH<sub>2</sub>)<sub>15</sub>CH<sub>3</sub>], 1.25 [56H, m, CH<sub>2</sub>(CH<sub>2</sub>)<sub>14</sub>CH<sub>3</sub>],  $\approx$ 1.8 [3H, m, CH(CH<sub>3</sub>)], 3.32 [4H, t, NCH<sub>2</sub>], 5.03 [1H, m, CH(CH<sub>3</sub>)], 7.30 [2H, m, CONH and pyridine-5H], 7.99 [1H, d, pyridine-4H], 8.60 [1H, d, pyridine-6H], and 9.00 [1H, s, pyridine-2H].

**6-Chlorohexyltrimethylammonium Bromide.** A mixture of 30% aqueous trimethylamine (5.6 g, 28 mmol), 1-bromo-6-chlorohexane<sup>10)</sup> (5.7 g, 29 mmol), and methanol (20 ml) was stirred for 40 h at room temperature. After evaporation of the solvent *in vacuo*, the residue was dissolved in water (20 ml) and washed with ether (2×20 ml). Evaporation to dryness gave a white solid: yield 5.0 g (68%), mp 113–114°C; <sup>1</sup>H-NMR (D<sub>2</sub>O, DSS)  $\delta$ =1.0–2.1 [8H, m, CH<sub>2</sub>(CH<sub>2</sub>)<sub>4</sub>CH<sub>2</sub>], 3.07 [9H, s, (CH<sub>3</sub>)<sub>3</sub>N<sup>+</sup>], 3.33 [2H, t, N<sup>+</sup>CH<sub>2</sub>], and 3.58 [2H, t, CH<sub>2</sub>Cl].

*N,N*-Dihexadecyl-*N*<sup>a</sup>-[1-(6-trimethylammoniohexyl)pyridinium-3-ylcarbonyl]-L-alaninamide Chloride Bromide [*N*<sup>+</sup>-C<sub>6</sub>(NA<sup>+</sup>)Ala2C<sub>16</sub>]. A mixture of (NA)Ala2C<sub>16</sub> (4.5 g, 6.9 mmol) and 6-chlorohexyltrimethylammonium bromide (3.5 g, 14 mmol) in dry *N,N*-dimethylformamide (10 ml) was stirred for 17 h at 120°C under nitrogen. After the mixture was cooled to room temperature, the solvent was removed *in vacuo*, and the crude product was purified by gel-filtration chromatography on columns of Sephadex LH-20 and Toyopearl HW-40 fine in this sequence with methanol as an eluant: a pale brown glassy solid, yield 3.0 g (47%); <sup>1</sup>H-NMR (CDCl<sub>3</sub>, TMS)  $\delta$ =0.88 [6H, t, (CH<sub>2</sub>)<sub>15</sub>CH<sub>3</sub>], 1.26 [64H, m, CH<sub>2</sub>(CH<sub>2</sub>)<sub>14</sub>CH<sub>3</sub> and N<sup>+</sup>CH<sub>2</sub>(CH<sub>2</sub>)<sub>4</sub>CH<sub>2</sub>],  $\approx$ 1.6 [3H, m, CH(CH<sub>3</sub>)], 2.8–3.7 [6H, m, NCH<sub>2</sub> and (CH<sub>3</sub>)<sub>3</sub>N<sup>+</sup>CH<sub>2</sub>], 3.34 [9H, s, (CH<sub>3</sub>)<sub>3</sub>N<sup>+</sup>], 4.90 [3H, m, N<sup>+</sup>(CH<sub>2</sub>)<sub>5</sub>CH<sub>2</sub> and CH(CH<sub>3</sub>)], 8.23 [1H, t, pyridine-5H], 8.95 [1H, d, pyridine-4H], 9.50 [1H, m, CONH], 9.90 [1H, d, pyridine-6H], and 10.38 [1H, s, pyridine-2H].

Found: C, 67.00; H, 10.37; N, 6.34%. Calcd for C<sub>50</sub>H<sub>96</sub>BrClN<sub>4</sub>O<sub>2</sub>: C, 66.68; H, 10.72; N, 6.22%.

*N,N*-Dihexadecyl-*N*<sup>a</sup>-[1-(6-trimethylammoniohexyl)-1,4-dihydro-3-pyridylcarbonyl]-L-alaninamide Bromide [*N*<sup>+</sup>-C<sub>6</sub>(NAH)-Ala2C<sub>16</sub>].

A solution of *N*<sup>+</sup>-C<sub>6</sub>(NA<sup>+</sup>)Ala2C<sub>16</sub> (140 mg, 0.16 mmol) and 1-benzyl-1,4-dihydronicotinamide<sup>11)</sup> (280 mg, 1.3 mmol) in dry methanol (2 ml) was placed in an ice bath, protected from room light, and stirred for 1 h under nitrogen atmosphere. The product was purified by gel-filtration chromatography on a column of Toyopearl HW-40 superfine with dry methanol as an eluant: a yellow solid, yield 40 mg (31%);  $\lambda_{\max}$  (methanol) 356 nm ( $\epsilon$  6000); <sup>1</sup>H-NMR (CDCl<sub>3</sub>, TMS)  $\delta$ =0.88 [3H, t, (CH<sub>2</sub>)<sub>15</sub>CH<sub>3</sub>], 1.26 [64H, m, CH<sub>2</sub>(CH<sub>2</sub>)<sub>14</sub>CH<sub>3</sub> and N<sup>+</sup>CH<sub>2</sub>(CH<sub>2</sub>)<sub>4</sub>CH<sub>2</sub>],  $\approx$ 1.8 [3H, m, CH(CH<sub>3</sub>)], 2.8–3.7 [10H, m, NCH<sub>2</sub>, N<sup>+</sup>CH<sub>2</sub>(CH<sub>2</sub>)<sub>4</sub>CH<sub>2</sub>, and pyridine-4H], 3.38 [9H, s, (CH<sub>3</sub>)<sub>3</sub>N<sup>+</sup>], 4.80 [2H, m, CH(CH<sub>3</sub>) and pyridine-5H], 5.65 [1H, d, pyridine-6H], 6.25 [1H, d, CONH], and 6.88 [1H, s, pyridine-2H].

Found: C, 70.26; H, 11.59; N, 6.48%. Calcd for C<sub>50</sub>H<sub>97</sub>BrN<sub>4</sub>O<sub>2</sub>: C, 69.33; H, 11.29; N, 6.47%.

The absence of chloride ion in the purified product was

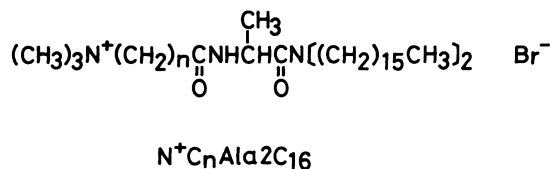
confirmed by qualitative analysis.<sup>12</sup> The product decomposed gradually in the air at room temperature. Therefore, freshly prepared samples were used for all the measurements. A 1,6-dihydronicotinamide isomer was obtained as a by-product in the hydrogen transfer reaction between a 1,4-dihydronicotinamide and its dehydrogenated species.<sup>13</sup> However, the 1,6-isomer of  $N^+C_6(NAH)Ala2C_{16}$  was not detected in the purified product by NMR analysis.

**Kinetic Measurements.** For the reduction of 2,6-dichloroindophenol (DCIP) and sodium 2,4,6-trinitrobenzenesulfonate (TNBS) with  $N^+C_6(NAH)Ala2C_{16}$  in aqueous media, the reaction rate was measured with the stopped-flow spectrophotometer. Single-compartment vesicles of the lipid ( $4.0 \times 10^{-4}$  mol dm<sup>-3</sup>) were prepared by injecting 50  $\mu$ l of an ethanol solution of the lipid into 5 ml of an aqueous phosphate buffer (0.01 mol dm<sup>-3</sup>, pH 7.1), while ethanol solutions of the substrates were mixed with the same buffer to give final substrate concentrations of  $4.0 \times 10^{-5}$  mol dm<sup>-3</sup> with the 1 (v/v)% ethanol content. Equal volumes of both vesicle and substrate solutions were rapidly mixed to initiate the reaction. The reaction was followed by monitoring the absorbance change at 600 nm (the absorption maximum for DCIP)<sup>14</sup> or 462 nm (the absorption maximum for the reduced form of TNBS).<sup>15</sup> As for the reduction of the substrates with 1-propyl-1,4-dihydronicotinamide (PNAH)<sup>16</sup> in the phosphate buffer (0.01 mol dm<sup>-3</sup>, pH 7.1, 50 (v/v)% ethanol), the reaction was relatively slow and the rate was measured with the ordinary spectrophotometer. The reduction of *N*-methylacridinium chloride, Malachite Green, and trifluoroacetophenone was monitored by the ordinary spectrophotometric method: the absorbance changes at 357 (the absorption maximum for *N*-methylacridinium chloride),<sup>17</sup> 617 (the absorption maximum for Malachite Green),<sup>18</sup> and 370 nm (the absorption due to the 1,4-dihydronicotinamide moiety)<sup>19</sup> were measured, respectively.

## Results and Discussion

**Morphology of Aggregates.** The peptide lipid bearing the 1,4-dihydronicotinamide moiety,  $N^+C_6(NAH)Ala2C_{16}$ , forms bilayer membranes in aqueous media. The phase transition parameters evaluated by

differential scanning calorimetry (DSC) for its aqueous dispersion are as follows:  $T_m$ , 19.5 °C;  $\Delta H$ , 33 kJ mol<sup>-1</sup> (Fig. 1a). This is consistent with the formation of multi-walled vesicles and/or lamellae. In the light of our previous study, these parameters are primarily manipulated by the size of the double alkyl-chain segment of peptide lipids. The parameters obtained for  $N^+C_6(NAH)Ala2C_{16}$  are in good agreement with those observed for peptide lipids having the same double chain segment such as  $N^+C_nAla2C_{16}$  ( $n=2, 5, 7$ , and 10).<sup>20</sup>



In order to prepare single-walled bilayer vesicles of  $N^+C_6(NAH)Ala2C_{16}$ , the injection method which was originally employed for the formation of single-walled liposomes<sup>21</sup> was adopted in this work to avoid degradation of the 1,4-dihydronicotinamide group, which was detected to occur spectrophotometrically under ordinary sonication conditions. The solution thus obtained was sufficiently clear for the following various measurements in contrast to the slightly turbid dispersion of the lipid.

The electronic absorption and fluorescence maxima of  $N^+C_6(NAH)Ala2C_{16}$  in ethanol at 15 °C were observed at 353 and 448 nm, respectively, and identical with those of 1-propyl-1,4-dihydronicotinamide (PNAH). Since these spectroscopic maxima for the 1,4-dihydronicotinamide moiety are much sensitive to the microenvironmental polarity, such polarity in the so-called hydrogen-belt domain of the single-walled vesicle was evaluated by referring to the corresponding spectra of PNAH in various media. As a result, the present hydrogen-belt domain with absorption and fluorescence maxima at 359.5 and 455 nm, respectively, provides a microenvironment equivalent to that provided by ethanol-water (1:1 v/v) (solvent polarity *Y*-parameter, 1.665).<sup>22</sup> In addition, the fluorescence polarization ( $P=0.317$ ) for the 1,4-dihydronicotinamide moiety of  $N^+C_6(NAH)Ala2C_{16}$  in the single-walled aggregate at 15 °C is larger than that measured in ethanol (0.114). This must be attributed to the tight side-by-side arrangement of the amphiphile molecules in the aggregated state.

An aqueous dispersion of  $N^+C_6(NA^+)Ala2C_{16}$ , the dehydrogenated counterpart of  $N^+C_6(NAH)Ala2C_{16}$ , shows a broad endothermic peak in the 5–20 °C range as shown in Fig. 1b. The morphological transformation of multi-walled bilayer aggregates, composed of natural and/or synthetic lipids, into smaller vesicles are reflected on the phase transition behavior between the gel and liquid-crystalline states; decrease in  $\Delta H$  along with peak-broadening and shift of  $T_m$  to lower temperature.<sup>20,23</sup> The DSC thermogram for an aqueous dispersion of  $N^+C_6(NA^+)Ala2C_{16}$  is almost comparable to that for a sonicated solution of  $N^+C_5Ala2C_{16}$ . This implies that dicationic amphi-

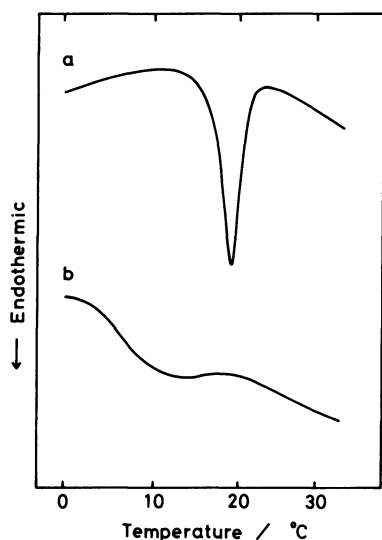


Fig. 1. DSC thermograms for aqueous dispersions of peptide lipids: a,  $N^+C_6(NAH)Ala2C_{16}$ ; b,  $N^+C_6(NA^+)Ala2C_{16}$ .

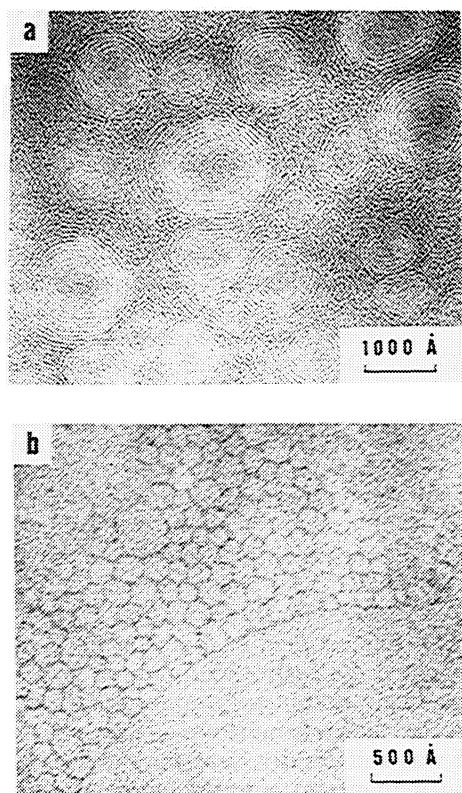
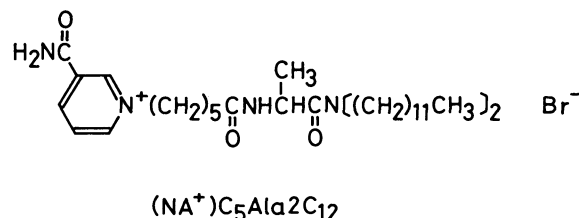


Fig. 2. Electron micrographs negatively stained with uranyl acetate: a, 10 mmol dm<sup>-3</sup> aqueous dispersion of N<sup>+</sup>C<sub>6</sub>(NA<sup>+</sup>)Ala2C<sub>16</sub>; b, 10 mmol dm<sup>-3</sup> aqueous solution of N<sup>+</sup>C<sub>6</sub>(NA<sup>+</sup>)Ala2C<sub>16</sub> sonicated for 2 min at 30 W.

philes are inclined to form smaller aggregates compared with those of the corresponding monocationic ones having the same double alkyl chains when they are dispersed in water. Indeed, the electron micrograph of an aqueous dispersion of N<sup>+</sup>C<sub>6</sub>(NA<sup>+</sup>)Ala2C<sub>16</sub> shows the presence of multi-walled vesicles with 500–1500 Å diameter (Fig. 2a) without forming straight or bent lamellae observed for aqueous dispersions of N<sup>+</sup>C<sub>n</sub>Ala2C<sub>16</sub> ( $n=2, 5, 7$ , and 10).<sup>20</sup> The difference in aggregate morphology is apparently due to the extensive electrostatic repulsion among the N<sup>+</sup>C<sub>6</sub>(NA<sup>+</sup>)Ala2C<sub>16</sub> molecules in the aggregated state. Sonication of an aqueous dispersion of N<sup>+</sup>C<sub>6</sub>(NA<sup>+</sup>)Ala2C<sub>16</sub> with a probe-type sonicator for 2 min at 30 W resulted in a clear solution state which gave an electron micrograph indicating the presence of small particles in a manner as observed for sonicated solutions of N<sup>+</sup>C<sub>n</sub>Ala2C<sub>16</sub><sup>20</sup> (Fig. 2b).

We have reported previously that an amphiphile involving the nicotinamide moiety as a polar head group, *N,N*-didodecyl-*N*<sup>α</sup>-[6-(3-carbamoylpyridinio)hexanoyl]-L-alaninamide bromide [(NA<sup>+</sup>)C<sub>5</sub>Ala2C<sub>12</sub>], forms single-compartment vesicles in aqueous media upon sonication and provides molecular organization much favorable for the formation of charge-transfer (CT) complexes with electron donors such as 3-indolylacetic acid.<sup>24</sup> The CT interaction of N<sup>+</sup>C<sub>6</sub>(NA<sup>+</sup>)Ala2C<sub>16</sub> (sonicated in water) with 3-indol-



ylacetic acid was quite effective and showed the biphasic CT complex formation in a manner as observed with the vesicular system composed of (NA<sup>+</sup>)C<sub>5</sub>Ala2C<sub>12</sub>. The formation constant for the CT complex thus obtained on a 2:1 (nicotinamide *vs.* 3-indolylacetic acid) stoichiometry is 7.3×10<sup>3</sup> mol<sup>-1</sup> dm<sup>3</sup> at 25 °C in water.<sup>25</sup> Thus, it is reasonable to consider that such CT interaction is also effective for the vesicular system composed of N<sup>+</sup>C<sub>6</sub>(NAH)Ala2C<sub>16</sub>, the 1,4-dihydronicotinamide moiety being the CT donor. Hence, the highly organized molecular aggregates formed with N<sup>+</sup>C<sub>6</sub>(NAH)Ala2C<sub>16</sub> and its dehydrogenated counterpart are expected to be utilized as effective reaction sites capable of promoting redox reactions due to the so-called proximity effect when substrate species, acting as CT-acceptors or -donors, are incorporated into them.

#### Reactivity of N<sup>+</sup>C<sub>6</sub>(NAH)Ala2C<sub>16</sub> Membrane in the Reduction of Various Substrates.

In order to evaluate the reactivity of N<sup>+</sup>C<sub>6</sub>(NAH)Ala2C<sub>16</sub> membrane prepared by the injection method, the following substrates were used: cationic, *N*-methylacridinium chloride and Malachite Green; nonionic trifluoroacetophenone; anionic, 2,6-dichloroindophenol (DCIP) and sodium 2,4,6-trinitrobenzenesulfonate (TNBS). The reactions were carried out in an aqueous phosphate buffer (0.01 mol dm<sup>-3</sup>, pH 7.1) containing 1 (v/v)% ethanol. In general, the reaction rate for reduction with NAD(P)H models is much influenced by the nature of microenvironment where the reaction takes place.<sup>17,26</sup> Prior to the kinetic analysis of the substrate-binding process with the membrane and the subsequent reduction, a reference reaction was examined in a homogeneous solution which provides the polarity equivalent to that in the N<sup>+</sup>C<sub>6</sub>(NAH)Ala2C<sub>16</sub> membrane: the hydrogenation with PNAH was investigated in ethanol-water (1:1 v/v).

As for the reduction of the cationic and neutral substrates, each substrate underwent reaction at an identical rate regardless of the nature of media, ethanol-water or membrane. This implies that the electrostatic repulsion on the positively charged surface of the membrane toward the cationic substrates inhibits the effective incorporation of the substrates into the membrane while the hydrophobic interaction between the hydrophobic domain of the membrane and the neutral substrate disturbs to attain the effective substrate concentration in the hydrogen-belt domain.

As for the reduction of the anionic substrates, however, the marked rate acceleration was observed in the membrane system. As shown in Table 1, the reaction rates for the reduction of DCIP and TNBS in the bilayer membrane were enhanced by 72- and 1.1×10<sup>5</sup>-fold, respectively, relative to those in ethanol-water

TABLE 1. APPARENT FIRST-ORDER RATE CONSTANTS FOR THE REDUCTION OF 2,6-DICHLOROINDOPHENOL (DCIP) AND SODIUM 2,4,6-TRINITROBENZENESULFONATE (TNBS) WITH 1,4-DIHYDRONICOTINAMIDE DERIVATIVES AT 15.0 °C<sup>a</sup>)

Substrate	1,4-Dihydronicotinamide	Medium <sup>b</sup> )	$k_{\text{obsd}}/\text{s}^{-1}$
DCIP	N <sup>+</sup> C <sub>6</sub> (NAH)Ala2C <sub>16</sub> <sup>c</sup> )	A	$9.4 \times 10^{-1}$
DCIP	PNAH	B	$1.3 \times 10^{-2}$
TNBS	N <sup>+</sup> C <sub>6</sub> (NAH)Ala2C <sub>16</sub> <sup>c</sup> )	A	2.5
TNBS	PNAH	B	$2.3 \times 10^{-5}$

a) Initial concentrations: 1,4-dihydronicotinamide derivatives,  $2.0 \times 10^{-4} \text{ mol dm}^{-3}$ ; substrates,  $2.0 \times 10^{-5} \text{ mol dm}^{-3}$ .

b) A, phosphate buffer (0.01 mol dm<sup>-3</sup>, pH 7.1) containing 1 (v/v)% ethanol; B, phosphate buffer (0.01 mol dm<sup>-3</sup>, pH 7.1) containing 50 (v/v)% ethanol. c) Single-walled vesicles.

(1:1 v/v). Although the high reactivity of both of the anionic substrates in the membrane is undoubtedly due to the favorable electrostatic interaction which takes the substrates in the membrane surface, other interaction modes, which take the substrates into the hydrogen-belt domain, must be operative. Before such effects are discussed, the kinetic analysis needs to be carried out on the basis of the pseudo-phase concept<sup>27,28)</sup> which was originally adopted for the analysis of micellar reactions.

According to the Berezin's concept which quantitatively explain the micellar effect on a bimolecular reaction,<sup>27)</sup> the pseudo-first-order rate constant,  $k_{\text{obsd}}$ , is given by the following equation:

$$k_{\text{obsd}} = \frac{k_m P_{\text{TNBS}} P_{\text{NAH}} C \bar{V} + k_w (1 - C \bar{V})}{[1 + (P_{\text{TNBS}} - 1) C \bar{V}][1 + (P_{\text{NAH}} - 1) C \bar{V}]} [\text{NAH}]_0 \quad (2)$$

Here,  $k_m$  and  $k_w$  represent the second-order rate constants in the bilayer membrane and in water, respectively;  $P_{\text{TNBS}}$  and  $P_{\text{NAH}}$  denote the partition coefficients of TNBS and N<sup>+</sup>C<sub>6</sub>(NAH)Ala2C<sub>16</sub>, respectively, between the membrane and water, e.g.,  $P_{\text{TNBS}} = [\text{TNBS}]_m / [\text{TNBS}]_w$  where the subscripts, m and w, stand for the membrane and water phases, respectively;  $\bar{V}$  is the partial molar volume of the lipid in the membrane;  $C$  designates the stoichiometric lipid concentration minus its critical aggregate concentration (CAC); and  $[\text{NAH}]_0$  is the total lipid concentration. Under the present kinetic conditions, the following assumptions are valid: (i) the rate of reaction in water is neglected, i.e.,  $k_m P_{\text{TNBS}} P_{\text{NAH}} C \bar{V} \gg k_w (1 - C \bar{V})$ ; (ii) the  $(1 - C \bar{V})$  term approximately equals 1 because of the low lipid concentration; (iii)  $C$  is nearly equals  $[\text{NAH}]_0$  and  $P_{\text{NAH}} C \bar{V} \gg 1$  because of the extremely low CAC;<sup>29)</sup> (iv) the binding constant for incorporation of TNBS into the N<sup>+</sup>C<sub>6</sub>(NAH)Ala2C<sub>16</sub> membrane, defined by  $K_{\text{TNBS}} = (P_{\text{TNBS}} - 1) \bar{V}$ , nearly equals  $P_{\text{TNBS}} \bar{V}$  because of  $P_{\text{TNBS}} \gg 1$ . Thus, Eq. 2 may be simplified to Eq. 3, which is subsequently rearranged to give Eq. 4.

$$k_{\text{obsd}} = \frac{k_m K_{\text{TNBS}} [\text{NAH}]_0}{\bar{V} (1 + K_{\text{TNBS}} [\text{NAH}]_0)} \quad (3)$$

$$\frac{1}{k_{\text{obsd}}} = \frac{\bar{V}}{k_m K_{\text{TNBS}} [\text{NAH}]_0} + \frac{\bar{V}}{k_m} \quad (4)$$

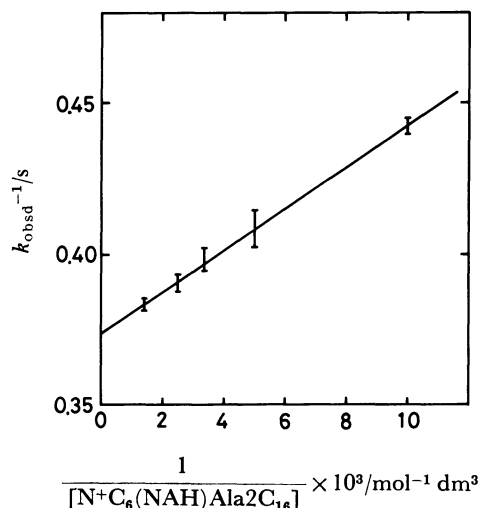


Fig. 3. Kinetic analysis on the basis of Eq. 4 for the reduction of TNBS with N<sup>+</sup>C<sub>6</sub>(NAH)Ala2C<sub>16</sub> membrane in a phosphate buffer (0.01 mol dm<sup>-3</sup>, pH 7.1) containing 1 (v/v)% ethanol at 15.0°C.

The plot of  $1/k_{\text{obsd}}$  vs.  $1/[\text{NAH}]_0$  gave a straight line correlation as illustrated in Fig. 3, and the  $K_{\text{TNBS}}$  value determined from its intercept and slope is  $5.5 \times 10^4 \text{ mol}^{-1} \text{ dm}^3$ . If one may employ  $0.75 \text{ mol}^{-1} \text{ dm}^3$  for the  $\bar{V}$  value, which is calculated from the volume per lipid molecule for egg yolk phosphatidylcholine vesicles,<sup>30)</sup> the second-order rate constant in the membrane is  $2.0 \text{ mol}^{-1} \text{ dm}^3 \text{ s}^{-1}$ . This assumption for  $\bar{V}$  is reasonable since all the average vesicle parameters for single-walled vesicles of N<sup>+</sup>C<sub>5</sub>Ala2C<sub>16</sub> and egg lecithin are comparable to each other as reported previously.<sup>20)</sup> The second-order rate constant in the present membrane is 17-fold greater than the corresponding value in the homogeneous solution ( $0.115 \text{ mol}^{-1} \text{ dm}^3 \text{ s}^{-1}$ ). Consequently, the marked overall rate enhancement observed for the reduction of TNBS primarily originates in the effective substrate incorporation into the hydrogen-belt domain of the membrane. Such efficient binding behavior may come from the three interaction modes: (i) the electrostatic attraction which takes the substrate molecules in the membrane surface, (ii) the CT interaction between the 1,4-dihydronicotinamide and the substrate, and (iii) the hydrogen bonding interaction between the substrate and the hydrogen-belt domain. The latter two interactions may act to translocate the substrate molecules from the membrane surface to the hydrogen-belt domain.

In conclusion, the bilayer membrane formed with the cationic peptide lipid bearing the 1,4-dihydronicotinamide moiety, N<sup>+</sup>C<sub>6</sub>(NAH)Ala2C<sub>16</sub>, acts as a potential reductant toward anionic substrates in aqueous media. The high reactivity primarily originates in the effective binding of such substrates to the lipid membrane, which is brought about by the three different interaction modes as stated above. The side-by-side arrangement of the 1,4-dihydronicotinamide moieties in the hydrogen-belt domain of the membrane may contribute in part to the overall

rate enhancement due to the proximity effect brought about by the CT and hydrogen-bonding interactions.

## References

- 1) J. H. Fendler, "Membrane Mimetic Chemistry," John Wiley & Sons, New York (1982), Chap. 6.
- 2) R. B. Gennis and A. Jonas, *Annual Rev. Biophys. Bioeng.*, **6**, 195 (1977).
- 3) Y. Murakami, A. Nakano, and K. Fukuya, *J. Am. Chem. Soc.*, **102**, 4253 (1980); Y. Murakami, Y. Aoyama, A. Nakano, T. Tada, and K. Fukuya, *ibid.*, **103**, 3951 (1981).
- 4) Y. Murakami, A. Nakano, and H. Ikeda, *J. Org. Chem.*, **47**, 2137 (1982).
- 5) Y. Murakami, A. Nakano, A. Yoshimatsu, and K. Fukuya, *J. Am. Chem. Soc.*, **103**, 728 (1981); Y. Murakami, A. Nakano, and K. Akiyoshi, *Bull. Chem. Soc. Jpn.*, **55**, 3004 (1982); Y. Murakami, J. Kikuchi, A. Nakano, K. Akiyoshi, and T. Imori, *ibid.*, in press.
- 6) T. Azumi and S. P. McGlynn, *J. Chem. Phys.*, **37**, 2413 (1962).
- 7) G. Mooser, H. Schulman, and D. S. Sigman, *Biochemistry*, **11**, 1595 (1972).
- 8) K. T. Dishart and R. Levine, *J. Am. Chem. Soc.*, **78**, 2268 (1956).
- 9) This material was prepared by a procedure similar to that reported for the synthesis of *N,N*-didodecyl-*N*<sup>α</sup>-(*t*-butoxycarbonyl)-L-alaninamide.<sup>4)</sup>
- 10) S. A. Fusari, K. W. Greenlee, and J. B. Brown, *J. Am. Oil Chem. Soc.*, **28**, 416 (1951).
- 11) Y. Kurusu, K. Nakajima, and M. Okawara, *Kogyo Kagaku Zasshi*, **71**, 934 (1968).
- 12) T. Momose, Y. Ueda, and Y. Mukai, *Bunseki Kagaku*, **9**, 360 (1960).
- 13) H. Minato, T. Ito, and M. Kobayashi, *Chem. Lett.*, **1977**, 13.
- 14) K. Wallenfels and M. Gellrich, *Justus Liebigs Ann. Chem.*, **621**, 149 (1959).
- 15) L. C. Kurz and C. Frieden, *Biochemistry*, **16**, 5207 (1977).
- 16) P. Karrer and F. J. Stare, *Helv. Chim. Acta*, **20**, 418 (1937).
- 17) J. Hajdu and D. S. Sigman, *Biochemistry*, **16**, 2841 (1977).
- 18) H. Kitano, M. Katsukawa, and N. Ise, *Bioorg. Chem.*, **11**, 412 (1982).
- 19) J. J. Steffens and D. M. Chipman, *J. Am. Chem. Soc.*, **93**, 6694 (1971).
- 20) Y. Murakami, A. Nakano, A. Yoshimatsu, K. Uchitomi, and Y. Matsuda, *J. Am. Chem. Soc.*, in press.
- 21) S. Batzri and E. D. Korn, *Biochim. Biophys. Acta*, **298**, 1015 (1973); J. M. H. Kremer, M. W. J. v. d. Esker, C. Pathmamanoharan, and P. H. Wiersema, *Biochemistry*, **16**, 3932 (1977).
- 22) A. H. Fainberg and S. Winstein, *J. Am. Chem. Soc.*, **78**, 2770 (1956).
- 23) D. Papahadjopoulos, S. Hui, W. J. Vail, and G. Poste, *Biochim. Biophys. Acta*, **448**, 245 (1976); Y. Okahata, R. Ando, and T. Kunitake, *Ber. Bunsenges. Phys. Chem.*, **85**, 789 (1981).
- 24) Y. Murakami, Y. Aoyama, J. Kikuchi, K. Nishida, and A. Nakano, *J. Am. Chem. Soc.*, **104**, 2937 (1982).
- 25) For definition of the formation constant and the experimental method, see reference 24.
- 26) P. van Eikeren and D. L. Grier, *J. Am. Chem. Soc.*, **98**, 4655 (1976).
- 27) I. V. Berezin, K. Martinek, and A. K. Yatsimirskii, *Russ. Chem. Rev.*, **42**, 787 (1973).
- 28) J. H. Fendler and W. L. Hinze, *J. Am. Chem. Soc.*, **103**, 5439 (1981).
- 29) In general, CAC's for amphiphiles of this type are lower than  $2 \times 10^{-5}$  mol dm<sup>-3</sup>.<sup>3,24)</sup>
- 30) C. Huang and J. T. Mason, *Proc. Natl. Acad. Sci. U.S.A.*, **75**, 308 (1978).